Pathway-dependent quantitative self-assembly of a metastable Pd_6L_4 square-based pyramid promoted by template and assist anions

Tsukasa Abe,[1] Shinnosuke Horiuchi,[1] and Shuichi Hiraoka[1,*]

[1]Department of Basic Science, Graduate School of Arts and Sciences, The University of Tokyo, Tokyo 153-8902, Japan.

*Correspondence: hiraoka-s@g.ecc.u-tokyo.ac.jp

Abstract

Precise control of molecular self-assembly process is one of ultimate goals in molecular self-assembly because this enables us to make a rational design of self-assembly pathway to selectively obtain even metastable assemblies, which is impossible under thermodynamic control. Toward this goal, modulation of the energy landscape of molecular self-assembly is demanded. Here, we report that a metastable ***Pd***$_6$L$_4$ square-based pyramid (SP) was almost quantitatively assembled by a pathway-dependent process with the aid of template and assist anions, which properly modulate the energy landscape, while usual heating a mixture of building blocks without modulation of the energy landscape gave a mixture of ***Pd***$_6$L$_4$ SP and uncharacterized species in equilibrium. These results indicate that synergy of template and assist effects is powerful approach for pathway selection in metal-organic assembly resulting in a metastable product selectively.

Introduction

Taking advantage of geometrically prescribed, relatively strong coordination bonds and high designability, metal-organic assembly has made great progress creating various well-defined discrete and infinite assembled structures (metal-organic cages[1–19] and metal-organic frameworks[20–32]) in the past few decades. Molecular self-assembly under thermodynamic control enables us to obtain thermodynamically most stable assembly efficiently thanks to error correction arising from the reversibility of interactions between the building blocks.[33,34] However, creation of metastable, complicated assemblies is still challenging in artificial molecular self-assembly. According to the laws of thermodynamics, metastable species cannot be produced as a major product under thermodynamic control, so kinetic approach is the only way to solve this problem.[35–71] But our understanding of energy landscapes of molecular self-assembly and their precise modulations is not sufficient for us to rationally design the assembly pathway through which a desired metastable assembly is selectively produced.

M_6L_4 square-based pyramid (SP) consisting of tritopic ligand **1** and $[Pd(en)]^{2+}$ (en: ethylenediamine) is a bowl-shaped structure assembled in D_2O originally reported by Fujita and coworkers.[72] In the course of our mechanistic study of the self-assembly process of the M_6L_4 SP, it was found that the self-assembly of tritopic ligand **1** and *cis*-protected $[\boldsymbol{Pd}Py^*_2]^{2+}$ complex (***Pd***: Pd(TMEDA), Py*: 3-chloropyridine) in organic solvent at relatively low concentration gave a mixture of the $[\boldsymbol{Pd}_2\mathbf{1}_2]^{4+}$ open structure, the $[\boldsymbol{Pd}_6\mathbf{1}_4]^{12+}$ SP, and uncharacterized species under thermodynamic control.[73] The $[\boldsymbol{Pd}_6\mathbf{1}_4]^{12+}$ SP is a dimerized structure of $[\boldsymbol{Pd}_2\mathbf{1}_2]^{4+}$ connected by two $\boldsymbol{Pd}^{2+}$ complexes (Fig. 1). The reason why the $[\boldsymbol{Pd}_6\mathbf{1}_4]^{12+}$ SP is not thermodynamically stable is mainly due to weak coordination bonds made between the two $[\boldsymbol{Pd}_2\mathbf{1}_2]^{4+}$ open structures (indicated as red broken circles in Fig. 1). Increasing the concentration of the substrates without competitive leaving ligand (Py*) shifts the equilibrium towards the $[\boldsymbol{Pd}_6\mathbf{1}_4]^{12+}$ SP but uncharacterized species remain even at almost saturation concentration (Figs. 1, left and S1).[73] Thus, the $[\boldsymbol{Pd}_6\mathbf{1}_4]^{12+}$ SP cannot be produced as a sole product under thermodynamic control.

Here we present almost quantitative assembly of the $[\boldsymbol{Pd}_6\mathbf{1}_4]^{12+}$ SP by pathway-dependent process under kinetic control promoted by synergy of the template anion (BF_4^-) and the assist anion (ReO_4^-) even at low concentration. These anions properly modulate the energy landscape of the self-assembly and enable to produce the metastable $[\boldsymbol{Pd}_6\mathbf{1}_4]^{12+}$ SP as a major product.

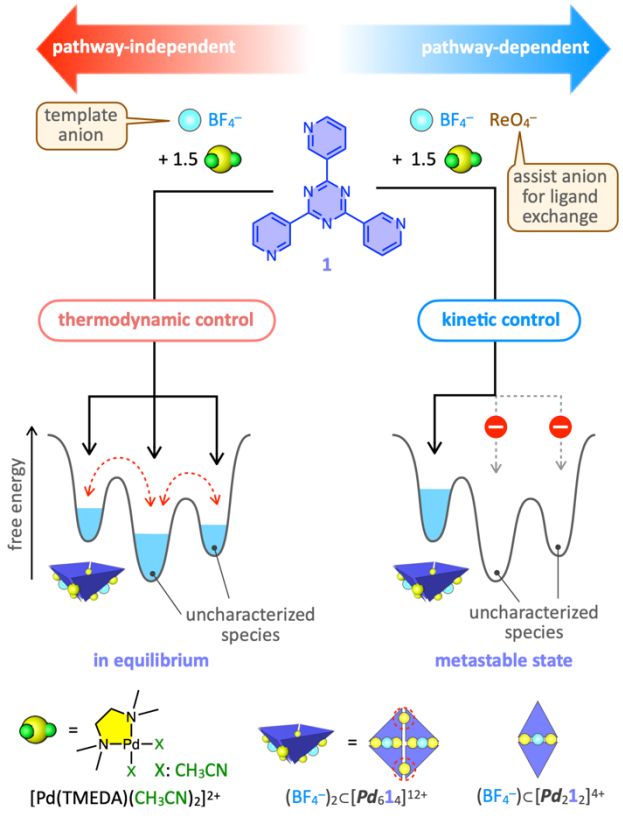

Figure 1. Pathway-dependent quantitative self-assembly of the metastable $[\boldsymbol{Pd}_6\mathbf{1}_4]^{12+}$ square-based pyramid (SP) through the $[\boldsymbol{Pd}_2\mathbf{1}_2]^{4+}$ open structure with the aid of template and assist anions (BF_4^- and ReO_4^-, respectively) under kinetic control (right). Usual thermodynamic approach by heating a mixture of building blocks ($\boldsymbol{Pd}^{2+}$ and **1** in a 3:2 ratio) led to a mixture of the $[\boldsymbol{Pd}_2\mathbf{1}_2]^{4+}$ open structure, the $[\boldsymbol{Pd}_6\mathbf{1}_4]^{12+}$ SP, and uncharacterized species in equilibrium (left). Red broken circles shown in $(BF_4^-)_2\subset[\boldsymbol{Pd}_6\mathbf{1}_4]^{12+}$ indicate weak Pd(II)–N coordination bonds, which affect the thermodynamic stability of the $(BF_4^-)_2\subset[\boldsymbol{Pd}_6\mathbf{1}_4]^{12+}$ SP.

Results and discussion

Thermodynamic properties of Pd_2L_2 open structure

It was recently found that a template anion is essential for the formation of the $[\mathbf{Pd_2 1_2}]^{4+}$ open structure to reduce electrostatic repulsion between the two Pd(II) ions.[34] PF_6^- is too large to be encapsulated, so $[\mathbf{Pd_2 1_2}]^{4+}$ cannot be formed with PF_6^- as the counter anion. Accordingly, we investigated the thermodynamic template effect[75–78] of anions on the self-assembly of $[\mathbf{Pd_2 1_2}]^{4+}$. Self-assembly of $(X^-)\subset[\mathbf{Pd_2 1_2}]^{4+}$ was carried out by mixing $\mathbf{Pd}^{2+}$ and **1** in a 1:1 ratio in the presence of anions smaller than PF_6^- (X^-: NO_3^-, BF_4^-, ClO_4^-, or ReO_4^-) under thermodynamic control (343 K) (Figs. 2a and S2). The yield of $(X^-)\subset[\mathbf{Pd_2 1_2}]^{4+}$ depended on the anion. NO_3^- led to the product in the highest yield (Fig. 2a), indicating that NO_3^- is the best template anion under thermodynamic control.

The ^{1}H NMR spectra of $(X^-)\subset[\mathbf{Pd_2 1_2}]^{4+}$ are almost the same except the chemical shift of H^a protons, which point towards the cavity of $[\mathbf{Pd_2 1_2}]^{4+}$, suggesting hydrogen bonds between anions (X^-) and H^a (Figs. 2b and S2). Lower down field shift of H^a proton of $(NO_3^-)\subset[\mathbf{Pd_2 1_2}]^{4+}$ than those of the other $(X^-)\subset[\mathbf{Pd_2 1_2}]^{4+}$ open structures suggests strong hydrogen bonds between H^a and NO_3^-.

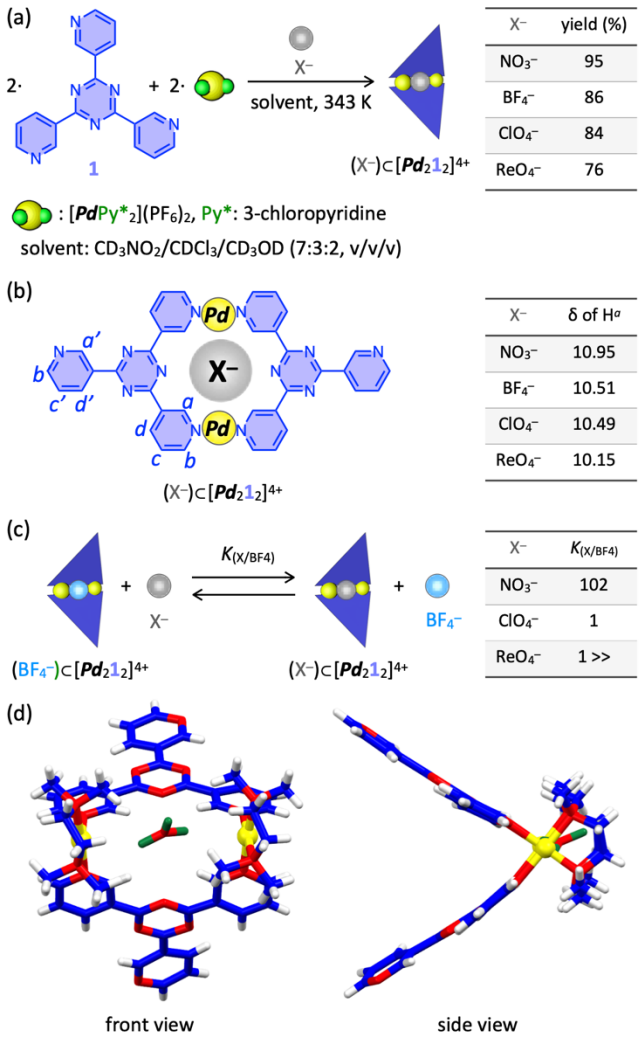

X⁻	yield (%)
NO_3^-	95
BF_4^-	86
ClO_4^-	84
ReO_4^-	76

X⁻	δ of H^a
NO_3^-	10.95
BF_4^-	10.51
ClO_4^-	10.49
ReO_4^-	10.15

X⁻	$K_{(X/BF4)}$
NO_3^-	102
ClO_4^-	1
ReO_4^-	1 >>

Figure 2. Thermodynamic properties of $(X^-)\subset[\mathbf{Pd_2 1_2}]^{4+}$ affected by the encapsulated anion (X^-). (a) The yields of $(X^-)\subset[\mathbf{Pd_2 1_2}]^{4+}$ under thermodynamic control, which were determined by ^{1}H NMR based on the internal standard. (b) The chemical shift values of H^a protons for $(X^-)\subset[\mathbf{Pd_2 1_2}]^{4+}$. (c) Relative affinity of X^- in the cavity of $[\mathbf{Pd_2 1_2}]^{4+}$ determined by competition experiments against BF_4^-. $K_{(X/BF4)}$ is defined as $([(X^-)\subset[\mathbf{Pd_2 1_2}]^{4+}][BF_4^-])/([(BF_4^-)\subset[\mathbf{Pd_2 1_2}]^{4+}][X^-])$. (d) The crystal structure of $(NO_3^-)\subset[\mathbf{Pd_2 1_2}]^{4+}$. Color labels, C: blue, N: red, O: green, Pd: yellow, H: white.

Colorless single crystals were obtained by slow diffusion of Et_2O into a solution of $(NO_3^-)\subset[\mathbf{Pd_2 1_2}](PF_6)_3$ in $CD_3NO_2/CDCl_3/CD_3OD$ prepared from **1** and $[\mathbf{Pd}Py^*_2](PF_6)_2$ with NO_3^-. The crystal structure of $(NO_3^-)\subset[\mathbf{Pd_2 1_2}](PF_6)_3$ (Fig. 2d and Table S1) showed that a NO_3^- anion was placed between the two positively charged Pd(II) ions, whose distance is 7.671 Å. Oxygen atoms of the bound NO_3^- and neighboring hydrogens (H^a in **1** and methyl groups of TMEDA) are closer than the sum of their van der Waals radii, indicating hydrogen bonds.

The relative affinity of the anions in the cavity of $[\mathbf{Pd_2 1_2}]^{4+}$ was evaluated by competition experiments (Figs. 2c and S3). NO_3^- is about 100 times more strongly bound to the cavity than BF_4^- and ClO_4^-, while the binding of ReO_4^- is much lower than that of BF_4^-. This binding preference reflects the size of the anions (NO_3^- < BF_4^- ≈ ClO_4^- < ReO_4^-) and does not consistent with the electrostatic surface potential of the anions (Fig. S4), so the size-complementarity is the dominant factor of the binding. The smallest NO_3^- is suitable to strongly bind in the cavity. The affinity of ReO_4^- is negligibly small, though ReO_4^- can work as a template of $[\mathbf{Pd_2 1_2}]^{4+}$ for its self-assembly.

Solvent also plays a key role to affect the energy landscape. Mixing of $[\mathbf{Pd}(CH_3CN)_2]^{2+}$ and **1** in a 1:1 ratio in the presence of coordinative solvent, $CD_3CN/CDCl_3/CD_3OD$ (7:3:2, v/v/v), at 298 K gave $(BF_4^-)\subset[\mathbf{Pd_2 1_2}]^{4+}$ in 76% yield and heating at 343 K decreased the yield of $(BF_4^-)\subset[\mathbf{Pd_2 1_2}]^{4+}$ (20%) with free **1** (53%) (Fig. S5). The self-assembly of the $(BF_4^-)_2\subset[\mathbf{Pd_6 1_4}]^{12+}$ SP from $[\mathbf{Pd}(CH_3CN)_2]^{2+}$ and **1** in a 3:2 ratio was also carried out in $CD_3CN/CDCl_3/CD_3OD$ (7:3:2, v/v/v) at 343 K resulting in no formation of the $(BF_4^-)_2\subset[\mathbf{Pd_6 1_4}]^{12+}$ SP (Fig. S6). These results indicate that $(BF_4^-)\subset[\mathbf{Pd_2 1_2}]^{4+}$ and the $(BF_4^-)_2\subset[\mathbf{Pd_6 1_4}]^{12+}$ SP are not thermodynamically most stable in coordinative solvent.

Kinetic effect of anions on the formation of Pd_2L_2 open structure

Template anions are expected not only to affect the thermodynamic stability of the assembly but also to affect the formation rate of the assembly (kinetic template effect[79–88]). The self-assembly of $(X^-)\subset[\mathbf{Pd_2 1_2}]^{4+}$ was monitored at 298 K by ^{1}H NMR spectroscopy (Figs. 3a and S7–S10). It was found that the formation of $(X^-)\subset[\mathbf{Pd_2 1_2}]^{4+}$ was very fast with NO_3^-, which is consistent with the strongest binding of NO_3^- in $[\mathbf{Pd_2 1_2}]^{4+}$. The self-assembly of $(ReO_4^-)\subset[\mathbf{Pd_2 1_2}]^{4+}$ is much faster than $(BF_4^-)\subset[\mathbf{Pd_2 1_2}]^{4+}$ and $(ClO_4^-)\subset[\mathbf{Pd_2 1_2}]^{4+}$ and comparable to $(NO_3^-)\subset[\mathbf{Pd_2 1_2}]^{4+}$, though the binding of ReO_4^- is much weaker than that of the other anions. This result suggests that fast formation of $(ReO_4^-)\subset[\mathbf{Pd_2 1_2}]^{4+}$ is caused due to acceleration of ligand exchanges by the participation of ReO_4^- in the ligand exchange process. The ligand exchanges on a Pd(II) ion center take place by associative mechanism[89–92] through a five-coordinate trigonal-bipyramidal transition state (Fig. 3b) and coordinative solvents and counter anions have potential to promote the ligand exchange process (assist effect).[93–95]

To truly evaluate the assist effect of the anions excluding the contribution of kinetic template effect, the self-assembly of the $[\mathbf{Pd_6 2_4}]^{12+}$ truncated tetrahedron (TT) from tritopic ligand **2** (2,4,6-tri(4-pyridyl)-1,3,5-triazine) was conducted under the same condition (Figs. S11-S13). The ^{1}H NMR spectrum of the $[\mathbf{Pd_6 2_4}]^{12+}$ TT was not affected by the anions (Figs. S11 and S12), indicating no interaction between the anion and the $[\mathbf{Pd_6 2_4}]^{12+}$ TT. Thus, NO_3^- and ReO_4^- do not play as a template in the self-assembly of the $[\mathbf{Pd_6 2_4}]^{12+}$ TT. The self-assembly of the $[\mathbf{Pd_6 2_4}]^{12+}$ TT was largely accelerated by NO_3^- and ReO_4^- compared with BF_4^- and the rate of the formation with NO_3^- is slightly

faster than with ReO_4^- (Fig. S13). Thus, NO_3^- plays as an excellent template (kinetic and thermodynamic template effects) and promotes ligand exchanges (assist effect), while ReO_4^- shows only good assist effect with very weak template effect for the self-assembly of $[\boldsymbol{Pd}_2\boldsymbol{1}_2]^{4+}$.

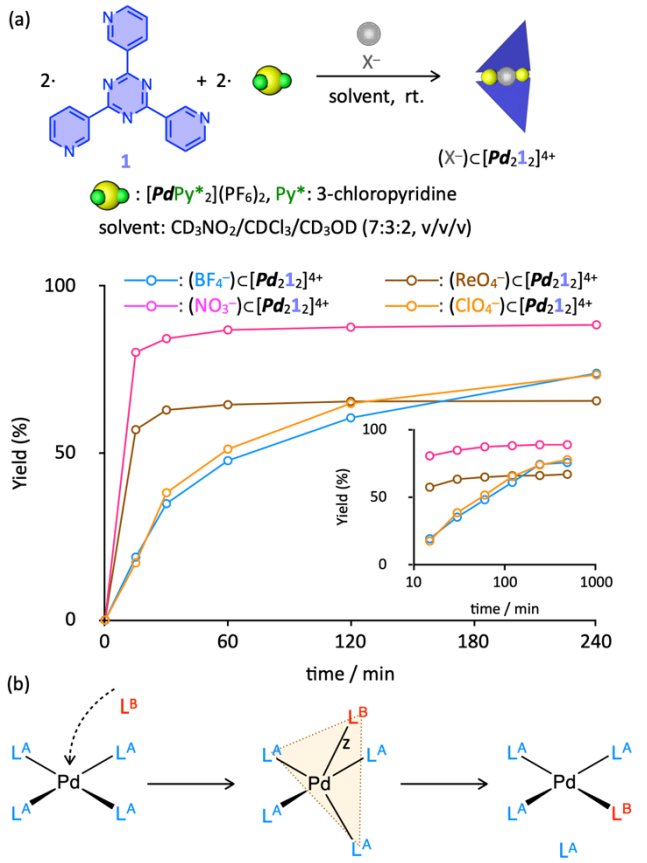

Figure 3. (a) Time-course of the self-assembly of $(X^-)\subset[\boldsymbol{Pd}_2\boldsymbol{1}_2]^{4+}$ at 298 K monitored by ^{1}H NMR spectroscopy ($[\boldsymbol{1}]_0$:$[\boldsymbol{Pd}]_0$:$[X^-]_0$ = 2:2:1). Inset indicates the logarithm plot. (b) Ligand exchange mechanism on a Pd(II) center by associative process. L^B indicates the entering ligand, which are the pyridyl groups in **1** and coordinative anions (NO_3^- and ReO_4^-) in the present case.

Kinetic assembly of $\boldsymbol{Pd_6L_4}$ SP from $\boldsymbol{Pd_2L_2}$ open structure

Encouraged by the good assist effect of NO_3^- and ReO_4^- and template effect of the anions in Fig. 2a, we were interested in modulation of the energy landscape by template and assist anions to obtain the metastable $[\boldsymbol{Pd}_6\boldsymbol{1}_4]^{12+}$ SP selectively. The possibility of pathway-dependent assembly of the $(X^-)_2\subset[\boldsymbol{Pd}_6\boldsymbol{1}_4]^{12+}$ SP was explored under various conditions (Fig. 4). It was found that the $(BF_4^-)_2\subset[\boldsymbol{Pd}_6\boldsymbol{1}_4]^{12+}$ SP was quantitatively produced from $(BF_4^-)\subset[\boldsymbol{Pd}_2\boldsymbol{1}_2]^{4+}$ and $\boldsymbol{Pd}^{2+}$ with ReO_4^- at 298 K in 1 h (Fig. 4b). The $(BF_4^-)_2\subset[\boldsymbol{Pd}_6\boldsymbol{1}_4]^{12+}$ SP thus obtained is kinetically stable enough not to be decomposed for at least 3 h at 343 K (Fig. S14). Observation of total 12 aromatic signals with the same integral values arising from desymmetrized tritopic ligand **1** (Fig. 4b) is consistent with the symmetry of the $[\boldsymbol{Pd}_6\boldsymbol{1}_4]^{12+}$ SP. The ^{1}H NMR signals of the $(BF_4^-)_2\subset[\boldsymbol{Pd}_6\boldsymbol{1}_4]^{12+}$ SP were assigned by (H,H)-COSY and (H,H)-NOESY spectroscopy (Figs. S15 and S16). The $(BF_4^-)_2\subset[\boldsymbol{Pd}_6\boldsymbol{1}_4]^{12+}$ SP was further characterized by ^{1}H DOSY spectroscopy (Fig. S17) and ESI-TOF spectrometry (Fig. S18). The ^{1}H NMR spectrum of the $(BF_4^-)_2\subset[\boldsymbol{Pd}_6\boldsymbol{1}_4]^{12+}$ SP in the presence of ReO_4^- is the same as that without ReO_4^- (Fig. S19), indicating that ReO_4^- does not interact with the $(BF_4^-)_2\subset[\boldsymbol{Pd}_6\boldsymbol{1}_4]^{12+}$ SP at all. Long time heating of a solution of the $(BF_4^-)_2\subset[\boldsymbol{Pd}_6\boldsymbol{1}_4]^{12+}$ SP at 343 K (9 days) gave a mixture of the $(BF_4^-)_2\subset[\boldsymbol{Pd}_6\boldsymbol{1}_4]^{12+}$ SP (30%) and uncharacterized species (70%), so the quantitatively formed $(BF_4^-)_2\subset[\boldsymbol{Pd}_6\boldsymbol{1}_4]^{12+}$ SP is a metastable state (Fig. 1, right).

In contrast, the yield of the $(BF_4^-)_2\subset[\boldsymbol{Pd}_6\boldsymbol{1}_4]^{12+}$ SP was quite low (61%) without ReO_4^- (Fig. S1), indicating that the assist effect of ReO_4^- dramatically promotes the formation of the metastable $(BF_4^-)_2\subset[\boldsymbol{Pd}_6\boldsymbol{1}_4]^{12+}$ SP. Interestingly, though NO_3^- has a greater assist ability, such a quantitative formation of the $[\boldsymbol{Pd}_6\boldsymbol{1}_4]^{12+}$ SP was not realized. The reaction of $(NO_3^-)\subset[\boldsymbol{Pd}_2\boldsymbol{1}_2]^{4+}$, $\boldsymbol{Pd}^{2+}$, and free NO_3^- at 298 K led to a mixture of the $(NO_3^-)_2\subset[\boldsymbol{Pd}_6\boldsymbol{1}_4]^{12+}$ SP (67%) and uncharacterized species (33%) (Fig. 4e). Heating this reaction mixture did not improve the yield of the $(NO_3^-)_2\subset[\boldsymbol{Pd}_6\boldsymbol{1}_4]^{12+}$ SP.

The $(NO_3^-)_2\subset[\boldsymbol{Pd}_6\boldsymbol{1}_4]^{12+}$ SP was obtained by exchange of BF_4^- in the $(BF_4^-)_2\subset[\boldsymbol{Pd}_6\boldsymbol{1}_4]^{12+}$ SP with NO_3^- (Fig. 4a). Several minor signals appeared after the formation of the $(NO_3^-)_2\subset[\boldsymbol{Pd}_6\boldsymbol{1}_4]^{12+}$ SP and the NMR spectrum finally became similar to that obtained from a mixture of $(NO_3^-)\subset[\boldsymbol{Pd}_2\boldsymbol{1}_2]^{4+}$ and $\boldsymbol{Pd}^{2+}$ (Figs. 4e and S20). These results indicate that the assist effect of NO_3^- is strong enough to rearrange the coordination bonds in the $(NO_3^-)_2\subset[\boldsymbol{Pd}_6\boldsymbol{1}_4]^{12+}$ SP resulting in equilibration of the system (Fig. 4).

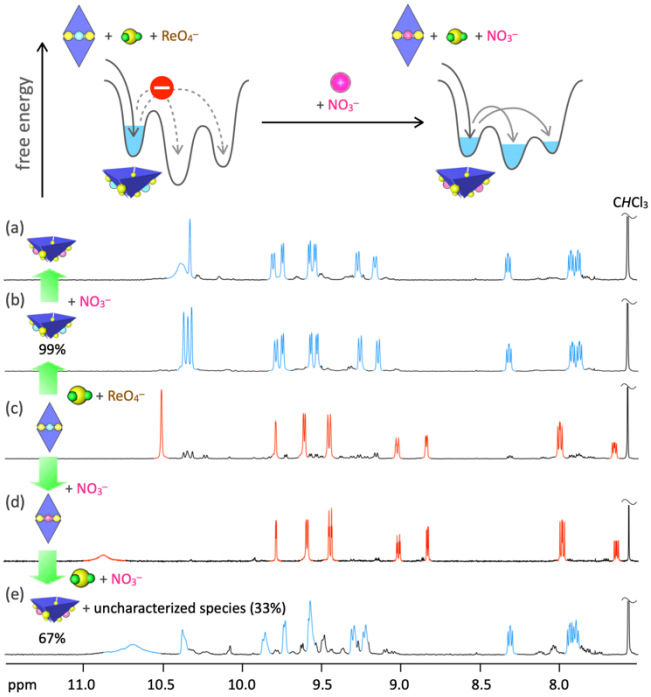

Figure 4. Pathway-dependent assembly of the $[\boldsymbol{Pd}_6\boldsymbol{1}_4]^{12+}$ SP from $(BF_4^-)\subset[\boldsymbol{Pd}_2\boldsymbol{1}_2]^{4+}$. Partial ^{1}H NMR spectra (500 MHz, $CD_3NO_2/CDCl_3/CD_3OD$ (7:3:2, v/v/v), 298 K, aromatic region) of (a) the $(NO_3^-)_2\subset[\boldsymbol{Pd}_6\boldsymbol{1}_4]^{12+}$ SP obtained immediately after the addition of NO_3^- in the $(BF_4^-)_2\subset[\boldsymbol{Pd}_6\boldsymbol{1}_4]^{12+}$ SP, (b) the $(BF_4^-)_2\subset[\boldsymbol{Pd}_6\boldsymbol{1}_4]^{12+}$ SP assembled from $(BF_4^-)\subset[\boldsymbol{Pd}_2\boldsymbol{1}_2]^{4+}$ and $\boldsymbol{Pd}^{2+}$ in the presence of ReO_4^-, (c) $(BF_4^-)\subset[\boldsymbol{Pd}_2\boldsymbol{1}_2]^{4+}$, (d) $(NO_3^-)\subset[\boldsymbol{Pd}_2\boldsymbol{1}_2]^{4+}$, and (e) the reaction mixture of $(NO_3^-)\subset[\boldsymbol{Pd}_2\boldsymbol{1}_2]^{4+}$ and $\boldsymbol{Pd}^{2+}$ in the presence of free NO_3^- measured after convergence at 298 K. Signals colored in red and blue indicate $(X^-)\subset[\boldsymbol{Pd}_2\boldsymbol{1}_2]^{4+}$ and the $(X^-)_2\subset[\boldsymbol{Pd}_6\boldsymbol{1}_4]^{12+}$ SP, respectively. Uncharacterized species were not observed by ^{1}H NMR spectroscopy. The yields were determined based on the internal standard. The assignment of the signals is shown in the Supporting Information.

Pathway-dependent quantitative self-assembly of $\boldsymbol{Pd_6L_4}$ SP

Finally, the direct formation of the $(BF_4^-)_2\subset[\boldsymbol{Pd}_6\boldsymbol{1}_4]^{12+}$ SP was conducted from **1** and $[\boldsymbol{Pd}(CH_3CN)_2](BF_4)_2$ with ReO_4^- (Fig. 1, right). Surprisingly, the $(BF_4^-)_2\subset[\boldsymbol{Pd}_6\boldsymbol{1}_4]^{12+}$ SP was obtained almost quantitatively (90%) in 3 h at 343 K in one step (Fig. 5b). The self-

assembly with only either BF_4^- or ReO_4^- gave the $(X^-)_2\subset[\boldsymbol{Pd_6}\boldsymbol{1}_4]^{12+}$ SP in 61% and 0% yield, respectively (Fig. S21). These results indicate that synergy of the template and assist anions modulate the energy landscape to make a proper self-assembly pathway to the metastable $(BF_4^-)_2\subset[\boldsymbol{Pd_6}\boldsymbol{1}_4]^{12+}$ SP.

Then, the pathway selection mechanism was preliminarily investigated. As the $(BF_4^-)_2\subset[\boldsymbol{Pd_6}\boldsymbol{1}_4]^{12+}$ SP was quantitatively produced from $(BF_4^-)\subset[\boldsymbol{Pd_2}\boldsymbol{1}_2]^{4+}$ and $\boldsymbol{Pd}^{2+}$ in the presence of ReO_4^- in 1 h (Fig. 4b), it is obvious that ReO_4^- significantly accelerates the dimerization of $(BF_4^-)\subset[\boldsymbol{Pd_2}\boldsymbol{1}_2]^{4+}$. In contrast, the formation of $(BF_4^-)\subset[\boldsymbol{Pd_2}\boldsymbol{1}_2]^{4+}$ was not accelerated by ReO_4^- (Fig. 5c). These results suggest that ReO_4^- mainly contributes to the dimerization of $(BF_4^-)\subset[\boldsymbol{Pd_2}\boldsymbol{1}_2]^{4+}$ with $\boldsymbol{Pd}^{2+}$ to form the $(BF_4^-)_2\subset[\boldsymbol{Pd_6}\boldsymbol{1}_4]^{12+}$ SP.

Based on these findings, the following scenario is proposed. First, BF_4^- promotes the formation of $(BF_4^-)\subset[\boldsymbol{Pd_2}\boldsymbol{1}_2]^{4+}$ by kinetic template effect but other intermediates are also produced. ReO_4^- largely accelerates the dimerization of $(BF_4^-)\subset[\boldsymbol{Pd_2}\boldsymbol{1}_2]^{4+}$ with $\boldsymbol{Pd}^{2+}$ to form the metastable $(BF_4^-)_2\subset[\boldsymbol{Pd_6}\boldsymbol{1}_4]^{12+}$ SP, which causes decrease in the concentration of $(BF_4^-)\subset[\boldsymbol{Pd_2}\boldsymbol{1}_2]^{4+}$. As $(BF_4^-)\subset[\boldsymbol{Pd_2}\boldsymbol{1}_2]^{4+}$ and other species are interconvertible by reversible reactions (Fig. 5a), low concentration of $(BF_4^-)\subset[\boldsymbol{Pd_2}\boldsymbol{1}_2]^{4+}$ would make a local equilibrium between $(BF_4^-)\subset[\boldsymbol{Pd_2}\boldsymbol{1}_2]^{4+}$ and other intermediates shift toward the formation of $(BF_4^-)\subset[\boldsymbol{Pd_2}\boldsymbol{1}_2]^{4+}$. $(BF_4^-)\subset[\boldsymbol{Pd_2}\boldsymbol{1}_2]^{4+}$ thus produced quickly reacts with $\boldsymbol{Pd}^{2+}$ to form the $(BF_4^-)_2\subset[\boldsymbol{Pd_6}\boldsymbol{1}_4]^{12+}$ SP by the assist effect of ReO_4^-. Relatively high kinetic stability of the $(BF_4^-)_2\subset[\boldsymbol{Pd_6}\boldsymbol{1}_4]^{12+}$ SP prevents the $(BF_4^-)_2\subset[\boldsymbol{Pd_6}\boldsymbol{1}_4]^{12+}$ SP from reaching thermodynamic equilibrium. If this mechanism is valid, ReO_4^- does not equally assist the ligand exchanges in all the elementary reactions concerning in the self-assembly. In other words, ReO_4^- seems to selectively modulate the dimerization step.

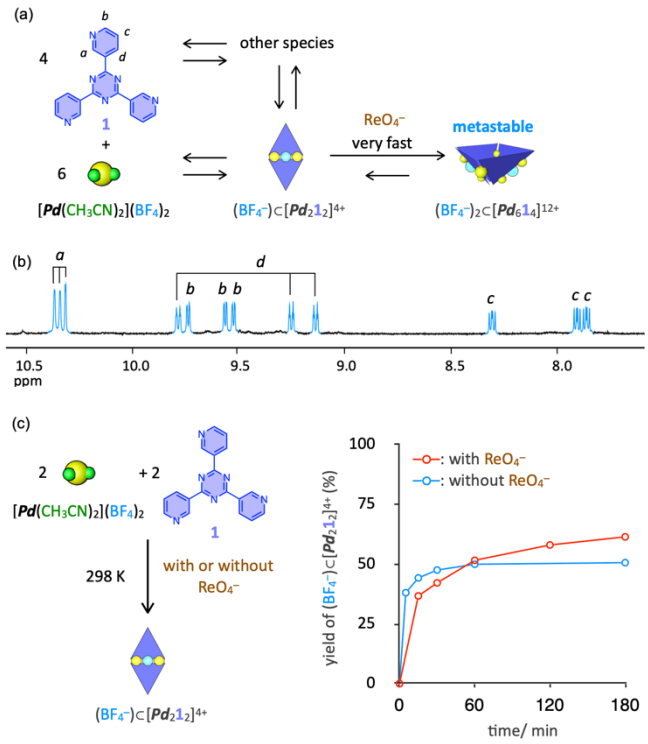

Figure 5. Direct self-assembly of the metastable $(BF_4^-)_2\subset[\boldsymbol{Pd_6}\boldsymbol{1}_4]^{12+}$ SP by synergy of template and kinetic effects. (a) A proposed mechanism of pathway selection in the self-assembly of the $(BF_4^-)_2\subset[\boldsymbol{Pd_6}\boldsymbol{1}_4]^{12+}$ SP. (b) A partial ^{1}H NMR (500 MHz, $CD_3NO_2/CDCl_3/CD_3OD$ (7:3:2, v/v/v), 298 K, aromatic region) of the $(BF_4^-)_2\subset[\boldsymbol{Pd_6}\boldsymbol{1}_4]^{12+}$ SP. Signals colored in blue are assigned to the $(BF_4^-)_2\subset[\boldsymbol{Pd_6}\boldsymbol{1}_4]^{12+}$ SP. The assignment of the signals was conducted based on (H,H)-COSY and (H,H)-NOESY spectroscopy (Figs. S15 and S16). (c) Self-assembly of $(BF_4^-)\subset[\boldsymbol{Pd_2}\boldsymbol{1}_2]^{4+}$ with or without ReO_4^-.

The yield of $(BF_4^-)\subset[\boldsymbol{Pd_2}\boldsymbol{1}_2]^{4+}$ was determined by ^{1}H NMR spectroscopy based on the internal standard.

Conclusion

In conclusion, a metastable assembly, the $(BF_4^-)_2\subset[\boldsymbol{Pd_6}\boldsymbol{1}_4]^{12+}$ SP, was almost quantitatively produced by pathway-dependent process under kinetic control. The pathway selection was realized by modulation of the energy landscape, which is affected by a combination of the template anion (BF_4^-), the assist anion (ReO_4^-), and solvent. Even though NO_3^- plays as both template and assistant for ligand exchange, the $[\boldsymbol{Pd_6}\boldsymbol{1}_4]^{12+}$ SP was not produced quantitatively with NO_3^- because its strong assist effect led the system to thermodynamic equilibrium. The preferential production of the metastable state was achieved by synergy of the template and assist effects with appropriate ability in almost non-coordinative solvent. The assist effect of ReO_4^- mainly contributes to the dimerization step of $(BF_4^-)\subset[\boldsymbol{Pd_2}\boldsymbol{1}_2]^{4+}$. Such a selective acceleration of a certain step(s) is the key to the pathway selection but its mechanism is unclear. More detailed investigation of the modulation of the energy landscape by quantitative analysis of self-assembly pathway[96,97] will reveal the origin of the synergistic effect on the pathway selection in molecular self-assembly. Further research along this line is currently underway.

Author contributions

S.Hi. conceived the project. T.A. carried out all experiments. S.Ho. conducted refinement of the crystal structure. S.Hi. prepared the manuscript and all authors discussed the results and commented on the manuscript.

Conflicts of interest

There are no conflicts to declare.

Acknowledgements

This work was supported by JSPS KAKENHI grant numbers 19H02731, 19K22196, and 21K18974 and the Asahi Glass Foundation.

References

1. D. L. Caulder, K. N. Raymond, Acc. Chem. Res. 1999, 32, 975–982.
2. M. Fujita, K. Umemoto, M. Yoshizawa, N. Fujita, T. Kusukawa, K. Biradha, *Chem. Commun.* **2001**, 509–518. DOI: doi.org/10.1039/B008684N
3. R. Chakrabarty, P. S. Mukherjee , P. J. Stang, *Chem. Rev.* **2011**, *111*, 6810–6918. DOI: 10.1021/cr200077m
4. K. Harris, D. Fujita, M. Fujita, *Chem. Commun.* **2013**, *49*, 6703–6712.
5. T. K. Ronson, S. Zarra, S. P. Black, J. R. Nitschke, *Chem. Commun.* **2013**, *49*, 2476–2490. DOI: 10.1039/C2CC36363A
6. T. R. Cook, P. J. Stang, *Chem. Rev.* **2015**, *115*, 7001–7045. DOI:
7. D. Fujita, Y. Ueda, S. Sato, N. Mizuno, T. Kumasaka, M. Fujita, *Nature* **2016**, *540*, 563–566. DOI: 10.1038/nature20771
8. Y. Fang, J. A. Powell, E. Li, Q. Wang, Z. Perry, A. Kirchon, X. Yang, Z. Xiao, C. Zhu, L. Zhang, F. Huang, H.-C. Zhou, Catalytic reactions within the cavity of coordination cages. *Chem. Soc. Rev.* **2019**, *48*, 4707–4730. DOI: 10.1039/C9CS00091G
9. Y. Inomata, T. Sawada, M. Fujita, *Chem* **2020**, *6*, 294–303. DOI: 10.1016/j.chempr.2019.12.009
10. E. G. Percástegui, T. K. Ronson, J. R. Nitschke, *Chem. Rev.* **2020**, *120*, 13480–13544. DOI: 10.1021/acs.chemrev.0c00672
11. Y. Sun, C. Chen, J. Liu, P. J. Stang, *Chem. Soc. Rev.* **2020**, *49*, 3889–3919. DOI: doi.org/10.1039/D0CS00038H
12. J. P. Carpenter, C. T. McTernan, J. L. Greenfield, R. Lavendomme, T. K. Ronson, J. R. Nitschke, *Chem* **2021**, *7*, 1534–1543. DOI: 10.1016/j.chempr.2021.03.005
13. D. Zhang, T. K. Ronson, Y.-Q. Zou, J. R. Nitschke, Metal–organic

cages for molecular separations. *Nat. Rev. Chem.* **2021**, *5*, 168–182. DOI: 10.1038/s41570-020-00246-1
14. T. Tateishi, M. Yoshimura, S. Tokuda, F. Matsuda, D. Fujita, S. Furukawa, Coordination/metal–organic cages inside out. *Coord. Chem. Rev.* **2022**, *467*, 214612. DOI: 10.1016/j.ccr.2022.214612
15. C. T. McTernan, J. A. Davies, J. R. Nitschke, *Chem. Rev.* **2022**, *122*, 10393–10437. DOI: 10.1021/acs.chemrev.1c00763
16. X.-Z. Li, C.-B. Tian, Q.-F. Sun, *Chem. Rev.* **2022**, *122*, 6374–6458. DOI: 10.1021/acs.chemrev.1c00602
17. R. Saha, B. Mondal, P. S. Mukherjee, Molecular cavity for catalysis and formation of metal nanoparticles for use in catalysis. *Chem. Rev.* **2022**, *122*, 12244–12307. DOI: 10.1021/acs.chemrev.1c00811
18. A. J. McConnell, *Chem. Soc. Rev.* **2022**, *51*, 2957–2971. DOI: 10.1039/D1CS01143J
19. A. Tarzia, K. E. Jelfs, Unlocking the computational design of metal–organic cages. *Chem. Commun.* **2022**, *58*, 3717–3730. DOI: 10.1039/d2cc00532h
20. B. F. Abrahams, B. F. Hoskins, D. M. Michail, R. Robson, Assembly of porphyrin building blocks into network structures with large channels. *Nature* **1994**, *369*, 727–729. DOI: 10.1038/369727a0
21. H. Li, M. Eddaoudi, M. O'Keeffe, O. M. Yaghi, Design and synthesis of an exceptionally stable and highly porous metal-organic framework. *Nature* **1999**, *402*, 276–279, DOI: 10.1038/46248
22. Yaghi O. M., O'Keeffe M., Ockwig N. W., Chae H. K., Eddaoudi M., Kim J., Reticular synthesis and the design of new materials. *Nature* **2003**, *423*, 705–714. DOI: 10.1038/nature01650
23. S. Kitagawa, R. Kitaura, S. Noro, Functional porous coordination polymers. *Angew. Chem. Int. Ed.* **2004**, *43*, 2334–2375. DOI: 10.1002/anie.200300610
24. A. J. Howarth, Y. Liu, P. Li, Z. Li, T. C. Wang, J. T. Hupp, O. K. Farha, Chemical, thermal and mechanical stabilities of metal-organic frameworks. *Nat. Rev. Mater.* **2016**, *1*, 1–15, DOI: 10.1038/natrevmats.2015.18
25. 2012 metal-organic frameworks issue. *Chem. Rev.* **2012**, *112*, 673–1268. http://pubs.acs.org/toc/chreay/112/2.
26. H. Furukawa, K. E. Cordova, M. O'Keeffe, M.; O. M. Yaghi, The chemistry and applications of metal-organic frameworks. *Science* **2013**, *341*, 1230444, DOI: 10.1126/science.1230444
27. Horike, S., Shimomura, S. & Kitagawa, S. Soft porous crystals. *Nat. Chem.* **2009**, *1*, 695–704. DOI: 10.1038/nchem.444
28. G. Ferey, Hybrid porous solids: past, present, future. *Chem. Soc. Rev.* **2008**, *37*, 191–214. DOI: 10.1039/B618320B
29. O. K. Farha, J. T. Hupp, Rational design, synthesis, purification, and activation of metal–organic framework materials. *Acc. Chem. Res.* **2010**, *43*, 1166–1175. DOI: 10.1021/ar1000617
30. M. O'Keeffe, O. M. Yaghi, Deconstructing the crystal structures of metal–organic frameworks and related materials into their underlying nets. *Chem. Rev.* **2012**, *112*, 675–702. DOI: 10.1021/cr200205j
31. M. L. Foo, R. Matsuda, S. Kitagawa, Functional hybrid porous coordination polymers. *Chem. Mater.* **2014**, *26*, 310–322. DOI: 10.1021/cm402136z
32. M. Eddaoudi, D. F. Sava, J. F. Eubank, K. Adil, V. Guillerm, Zeolite-like metal–organic frameworks (ZMOFs): design, synthesis, and properties. *Chem. Soc. Rev.* **2015**, *44*, 228–249. DOI: 10.1039/C4CS00230J
33. D. M. Whitesides, B. Grzybowski, Self-assembly at all scales. *Science* **2002**, *295*, 2418–2421. DOI : 10.1126/science.107082
34. J. M. Lehn, From supramolecular chemistry towards constitutional dynamic chemistry. *Chem. Soc. Rev.* **2007**, *36*, 151 – 160. DOI: 10.1039/B616752G
35. S. Tashiro, M. Tominaga, K. Kusukawa, M. Kawano, S. Sakamoto, K. Yamaguchi, M. Fujita, Pd^{II}-Directed dynamic assembly of a dodecapyridine ligand into end-capped and open tubes: The importance of kinetic control in self-assembly. *Angew. Chem. Int. Ed.* **2003**, *42*, 3267 – 3270. DOI: 10.1002/anie.200351397
36. H. Cui, Z. Chen, S. Zhong, K. L. Wooley, D. J. Pochan, Block copolymer assembly via kinetic control. *Science* **2007**, *317*, 647–650. DOI: 10.1126/science.1141768
37. P. Yin, H. M. T. Choi, C. R. Calvert, N. A. Pierce, Programming biomolecular self-assembly pathways. *Nature* **2008**, *451*, 318–322. DOI: 10.1038/nature06451
38. Y. Tidhar, H. Weissman, S. G. Wolf, A. Gulino, B. Rybtchinski, Pathway-dependent self-assembly of perylene diimide/peptide conjugates in aqueous medium. *Chem. Eur. J.* **2011**, *17*, 6068–6075. DOI: 10.1002/chem.201003419
39. O. Chepelin, J. Ujma, P. E. Barran, P. J. Lusby, Sequential, kinetically controlled synthesis of multicomponent stereoisomeric assemblies. *Angew. Chem. Int. Ed.* **2012**, *51*, 4194 – 4197. DOI: 10.1002/anie.201108994
40. Q. Lu, H. Zhu, C. Zhang, F. Zhang, B. Zhang, D. L. Kplan, Silk self-assembly mechanisms and control from thermodynamics to kinetics. *Biomacromolecules* **2012**, *13*, 826–832. DOI: 10.1021/bm201731e
41. M. D. Ward, P. R. Raithby, Functional behaviour from controlled self-assembly: Challenges and prospects. *Chem. Soc. Rev.* **2013**, 42, 1619–1636. DOI: 10.1039/C2CS35123D
42. J. Marti-Rujas, M. Kawano, Kinetic products in coordination networks: Ab initio X-ray powder diffraction analysis, *Acc. Chem. Res.* **2013**, *46*, 493–505. DOI: 10.1021/ar300212v
43. Y. Wang, R. Huang, W. Qi, Z. Wu, R. Su, Z. He, Kinetically controlled self-assembly of redox-active ferrocene-diphenylalanine: from nanospheres to nanofibers. *Nanotechnology* **2013**, *24*, 465603. DOI: 10.1088/0957-4484/24/46/465603
44. D. A. Roberts, A. M. Castilla, T. K. Ronson, J. R. Nitschke, Post-assembly modification of kinetically metastable $Fe^{II}_2L_3$ triple helicates." *J. Am. Chem. Soc.* **2014**, *136*, 8201–8204. DOI: 10.1021/ja5042397
45. D. Görl, X. Zhang, V. Stepanenko, F. Wurthner, Supramolecular block copolymers by kinetically controlled co-self-assembly of planar and core-twisted perylene bisimides. *Nat. Commun.* **2015**, *6*, 7009. DOI: 10.1038/ncomms8009
46. M. Numata, Supramolecular chemistry in microflow fields: Toward a new material world of precise kinetic control. *Chem. Asian J.* **2015**, *10*, 2574–2588. DOI: 10.1002/asia.201500555
47. T. Lin, Q. Wu, J. Liu, Z. Shi, P. N. Liu, N. Lin, Thermodynamic versus kinetic control in self-assembly of zero-, one-, quasi-two-, and two-dimensional metal-organic coordination structures. *J. Chem. Phys.* **2015**, *142*, 101909. DOI: 10.1063/1.4906174
48. D. van der Zwaag, T. F. de Greef, E. W. Meijer, Programmable supramolecular polymerizations. *Angew. Chem. Int. Ed.* **2015**, *54*, 8334–8336. DOI: 10.1002/anie.201503104
49. A. Aliprandi, M. Mauro, L. De Cola, Controlling and imaging biomimetic self-assembly. *Nat. Chem.* **2016**, *8*, 10–15. DOI: 10.1038/nchem.2383
50. Y. Yan, J. Huang, B. Z. Tang, Kinetic trapping– Strategy for directing the self-assembly of unique functional nanostructures. *Chem. Commun.* **2016**, *52*, 11870–11884. DOI: 10.1039/C6CC03620A
51. J. Wang, K. Liu, R. Xing, X. Yan, Peptide self-assembly: Thermodynamics and kinetics. *Chem. Soc. Rev.* **2016**, *45*, 5589–5604. DOI: 10.1039/C6CS00176A
52. T. Fukui, S. Kawai, S. Fujinuma, Y. Matsushita, T. Yasuda, T. Sakurai, S. Seki, M. Takeuchi, K. Sugiyasu, Control over differentiation of a metastable supramolecular assembly in one and two dimensions. *Nat. Chem.* **2017**, *9*, 493–499. DOI: 10.1038/nchem.2684
53. H. Ohtsu, M. Kawano, Kinetic assembly of coordination networks. *Chem. Commun.* **2017**, *53*, 8818–8829. DOI: 10.1039/C7CC04277A
54. L. Liu, G. Lyu, C. Liu, F. Jiang, D. Yuan, Q. Sun, K. Zhou, Q. Chen, M. Hong, Controllable reassembly of a dynamic metallocage: From thermodynamic control to kinetic control. *Chem. Eur. J.* **2017**, *23*, 456 – 461. DOI: 10.1002/chem.201604540
55. X. Zheng, L. Zhu, X. Zeng, L. Meng, L. Zhang, D. Wang, X. Huang, Kinetics-controlled amphiphile self-assembly processes. *Phys. Chem. Lett.* **2017**, *8*, 1798−1803. DOI: 10.1021/acs.jpclett.7b00160 J
56. C. Paris, A. Floris, S. Aeschlimann, J. Neff, F. Kling, A. Kuhnle, L. Kantorovich, Kinetic control of molecular assembly on surfaces. *Commun. Chem.* **2018**, *1*, 66. DOI: 10.1038/s42004-018-0069-0
57. X. Zhang, Y. Wang, Y. Hua, J. Duan, M. Chen, L. Wang, Z. Yang, Kinetic control over supramolecular hydrogelation and anticancer properties of taxol. *Chem. Commun.* **2018**, *54*, 755–758. DOI: 10.1039/C7CC08041G
58. T. Tateishi, S. Takahashi, A. Okazawa, V. Martí-Centelles, J. Wang, T. Kojima, P. J. Lusby, H. Sato, S. Hiraoka, Navigated self-assembly of a Pd_2L_4 cage by modulation of an energy landscape under kinetic control. *J. Am. Chem. Soc.* **2019**, *141*, 19669–19676. DOI: 10.1021/jacs.9b07779
59. G. Ben Messaoud, P. Le Griel, D. Hermida-Merino, S. L. K. W. Roelants, W. Soetaert, C. V. Stevens, N. Baccile, pH-Controlled self-

assembled fibrillar network hydrogels: Evidence of kinetic control of the mechanical properties. *Chem. Mater.* **2019**, *31*, 4817–4830. DOI: 10.1021/acs.chemmater.9b01230

60. L. H. Foianesi-Takeshige, S. Takahashi, T. Tateishi, R. Sekine, A. Okazawa, W. Zhu, T. Kojima, K. Harano, E. Nakamura, H. Sato, S. Hiraoka, Bifurcation of self-assembly pathways to sheet or cage controlled by kinetic template effect. *Commun. Chem.* **2019**, *2*, 128. DOI: 10.1038/s42004-019-0232-2
61. A.-L. Buckinx, K. Verstraete, E. Baeten, R. F. Tabor, A. Sokolova, N. Zaquen, T. Junkers, Kinetic control of aggregation shape in micellar self-assembly. *Angew. Chem. Int. Ed.* **2019**, *58*, 13799–13802. DOI: 10.1002/anie.201907371
62. M. Zangoli, M. Gazzano, F. Monti, L. Maini, D. Gentili, A. Liscio, A. Zanelli, E. Salatelli, G. Gigli, M. Baroncini, F. D. Maria, Thermodynamically versus kinetically controlled self-assembly of a naphthalenediimide−thiophene derivative: From crystalline, fluorescent, n-type semiconducting 1D needles to nanofibers. *ACS Appl. Mater. Interfaces* **2019**, *11*, 16864−16871. DOI: 10.1021/acsami.9b02404
63. M. A. VandenBerg, J. K. Sahoo, L. Zou, W. McCarthy, M. J. Webber, Divergent self-assembly pathways to hierarchically organized networks of isopeptide-modified discotics under kinetic control. *ACS Nano* **2020**, *14*, 5491−5505. DOI: 10.1021/acsnano.9b09610
64. H. Choi, S. Heo, S. Lee, K. Y. K. J. H. Lim, S. H. Jung, S. S. Lee, H. Miyake, J. Y. Lee, J. H. Jung, Kinetically controlled Ag+-coordinated chiral supramolecular polymerization accompanying a helical inversion. *Chem. Sci.* **2020**, *11*, 721–730. DOI: 10.1039/C9SC04958D
65. F. J. Rizzuto, J. R. Nitschke, Narcissistic, integrative, and kinetic self-sorting within a system of coordination cages. *J. Am. Chem. Soc.* **2020**, *142*, 7749–7753. DOI; 10.1021/jacs.0c02444
66. H. Kaur, R. Jain, S. Roy, Pathway-dependent preferential selection and amplification of variable self-assembled peptide nanostructures and their biological activities. *ACS Appl. Mater. Interfaces* **2020**, *12*, 52445−52456. DOI: 10.1021/acsami.0c16725
67. A. Ibáñez-Fonseca, D. Orbanic, F. J. Arias, M. Alonso, D. I. Zeugolis, J. C. Rodríguez-Cabello, Influence of the thermodynamic and kinetic control of self-assembly on the microstructure evolution of silk-elastin-like recombinamer hydrogels. *Small* **2020**, *16*, 2001244. DOI: 10.1002/smll.202001244
68. Z. Huang, T. Jiang, J. Wang, X. Ma, H. Tian, Real-time visual monitoring of kinetically controlled self-assembly. *Angew. Chem. Int. Ed.* **2021**, *60*, 2855–2860. DOI: 10.1002/anie.202011740
69. P.-P. Sun, B.-L. Han, H.-G. Li, C.-K. Zhang, X. Xin, J.-M. Dou, Z.-Y. Gao, D. Sun, Real-time fluorescent monitoring of kinetically controlled supramolecular self-assembly of atom-precise Cu8 nanocluster, *Angew. Chem. Int. Ed.* **2022**, *61*, e202200180. DOI: 10.1002/anie.202200180
70. M. Khodaverdi, M. S. Hossain, Z. Zhang, R. P. Martino, C. W. Nehls, D. Mozhdehi, Pathway-selection for programmable assembly of genetically encoded amphiphiles by thermal processing. *ChemSystemsChem* **2022**, *4*, e202100037. DOI: 10.1002/syst.202100037
71. J. Yang, L. Guo, X. Yong, T. Zhang, B. Wang, H. Song, Y. S. Zhao, H. Hou, B. Yang, J. Ding, S. Lu, Simulating the structure of carbon dots via crystalline π-aggregated organic nanodots prepared by kinetically trapped self-assembly. *Angew. Chem. Int. Ed.* **2022**, *61*, e202207817. DOI: 10.1002/anie.202207817
72. M. Fujita, S.-Y. Yu, T. Kusukawa, H. Funaki, K. Ogura, K. Yamaguchi, Self-assembly of nanometer-sized macrotricyclic complexes from ten small component molecules. *Angew. Chem. Int. Ed.* **1998**, *37*, 2082–2085. DOI: 10.1002/(SICI)1521-3773(19980817)37:15<2082::AID-ANIE2082>3.0.CO;2-0
73. T. Tateishi, S. Takahashi, I. Kikuchi, K. Aratsu, H. Sato, S. Hiraoka, Unexpected self-assembly pathway to a Pd(II) coordination square-based pyramid and its preferential formation beyond the boltzmann distribution, *Inorg. Chem.* **2021**, *60*, 16678−16685. DOI: 10.1021/acs.inorgchem.1c02570
74. T. Abe, S. Horiuchi, S. Hiraoka, Kinetically controlled narcissistic self-sorting of Pd(II)-linked self-assemblies from structurally similar tritopic ligands, *Chem. Commun.* **2022**, *58*, 10829–10832. DOI: 10.1039/d2cc04496j
75. M. C. Thompson, D. H. Busch, Reactions of coordinated ligands. IX. Utilization of the template hypothesis to synthesize macrocyclic ligands in Situ. *J. Am. Chem. Soc.* **1964**, *86*, 3651–3656. DOI: 10.1021/ja01072a012
76. B. Hasenknopf, J.-M. Lehn, N. Boumediene, A. Dupont-Gervais, A. Van Dorsselaer, B. Kneisel, D. Fenske, *J. Am. Chem. Soc.* **1997**, *119*, 10956–10962. DOI: 10.1021/ja971204r
77. J. D. Crowley, S. M. Goldup, A.-L. Lee, D. A. Leigh, R. T. McBurney, Active metal template synthesis of rotaxanes, catenanes and molecular shuttles. *Chem. Soc. Rev.* **2009**, *38*, 1530–1541. DOI: 10.1039/b804243h
78. J.-F. Ayme, J. E. Beves, C. J. Campbell, D. A. Leigh, Template synthesis of molecular knots. *Chem. Soc. Rev.* **2013**, *42*, 1700–1712. DOI: 10.1039/c2cs35229j
79. R. N. Green, 18-Crown-6: A strong complexing agent for alkalin metal cations. *Tetrahedron. Lett.* **1972**, *18*, 1793–1796. DOI: 10.1016/S0040-4039(01)85270-9
80. C. O. Dietrich-Buchecker, J.-P. Sauvage, J. P. Kintzinger, Une nouvelle famille de molecules : les metallo-catenanes. Tetrahedron Lett. 1983, 24, 5095–5098. DOI: 10.1016/S0040-4039(00)94050-4
81. T. J. McMuRRY, K. N. Raymond, P. H. Smith, Molecular Recognition and Metal Ion Template Synthesis. *Science*, **1989**, *244*, 938–943. DOI: 10.1126/science.2658057
82. S. Anderson, S. H. L. Anderson, J. K. M. Sanders, Expanding roles for templates in synthesis. *Acc. Chem. Res.* **1993**, *26*, 469–475. DOI:
83. R. Hoss, F. Vögtle, Template synthesis, *Angew. Chem. Int. Ed.* **1994**, *33*, 375-384.DOI: 10.1021/ar00033a003
84. P. Ghosh, O. Mermagen, C. A. Schalley, Novel template effect for the preparation of [2]rotaxanes with functionalised centre pieces. *Chem. Commun.* **2002**, 2628–2629. DOI: 10.1039/B208361B
85. D. A. Makeiff, D. J. Pope, J.C. Sherman, Template effects in the formation of a tetramethylene-bridged hemicarceplex. *J. Am. Chem. Soc.* **2000**, *122*, 1337–1342. DOI: 10.1021/ja9931628
86. T. J. Hubin, D. H. Busch, Template routes to interlocked molecular structures and orderly molecular entanglements. *Coord. Chem. Rev.* **2000**, 200–202, 5–52. DOI: 10.1016/S0010-8545(99)00242-8
87. M. S. Vickers, P. D. Beer, Anion templated assembly of mechanically interlocked structures. *Chem. Soc. Rev.* **2007**, *36*, 211–225. DOI: 10.1039/b518077p
88. S. Liu, D. V. Kondratuk, S. A. L. Rousseaux, G. Gil-Ramírez, M. C. O'Sullivan, J. Cremers, T.D. W. Claridge, H. L. Anderson, Caterpillar Track Complexes in Template-Directed Synthesis and Correlated Molecular Motion. *Angew. Chem. Int. Ed.* **2015**, *54*, 5355–5359. DOI: 10.1002/anie.201412293
89. F. Basolo, R. G. Pearson, *Mechanisms of Inorganic Reactions*, Wiley, New York, **1967**.
90. L. Canovese, L. Cattalini, P. Uguagliati, M. L. Tobe, The appearance of a stable intermediate in some substitution reactions of (1,5-diamino-3-azapentane)pyridinepalladium(II) perchlorate, *J. Chem. Soc. Dalton Trans.* **1990**, 867–872. DOI: 10.1039/DT9900000867
91. J. K. Burdett, Substitution reactions at square-planar d8 metal centers and the kinetic cis and trans effects. A general molecular orbital description, *Inorg. Chem.* **1977**, *16*, 3013–3025. DOI: 10.1021/ic50178a006
92. S. Kai, V. Martí-Centelles, Y. Sakuma, T. Mashiko, T. Kojima, U. Nagashima, M. Tachikawa, P. J. Lusby, S. Hiraoka, Quantitative analysis of self-assembly process of a Pd_2L_4 cage consisting of rigid ditopic ligands, *Chem. Eur. J.* **2018**, *24*, 663–671. DOI: 10.1002/chem.201704285
93. J. L. Walsh, C. C. Yancey, Acceleration of ligand exchange by coordinated nitrate in polypyridyl ruthenium complexes. *Polyhedron* **1989**, *8*, 1223–1226. DOI: 10.1016/S0277-5387(00)81144-4
94. S. Kai, Y. Sakuma, T. Mashiko, T. Kojima, M. Tachikawa, S. Hiraoka, The effect of solvent and coordination environment of metal source on the self-assembly pathway of a Pd(II)-mediated coordination capsule, *Inorg. Chem.* **2017**, *56*, 12652–12663. DOI: 10.1021/acs.inorgchem.7b02152
95. D. A. Poole, III, E. O. Bobylev, B. de Bruin, S. Mathew, J. N. H. Reek, Exposing mechanisms for defect clearance in supramolecular self-assembly: Palladium–pyridine coordination revisited. *Inorg. Chem.* **2023**, DOI: 10.1021/acs.inorgchem.2c04404
96. S. Hiraoka, S. Takahashi, H. Sato, Coordination self-assembly

processes revealed by collaboration of experiment and theory: Toward kinetic control of molecular self-assembly, *Chem. Rec.* **2021**, *21*, 443–459. DOI: 10.1002/tcr.202000124

97. Y. Tsujimoto, T. Kojima, S. Hiraoka, Rate-determining step in the self-assembly process of supramolecular coordination capsules. *Chem. Sci.* **2014**, *5*, 4167–4172. DOI: 10.1039/c4sc01652a